Adsorption/Desorption of Hydrogen on Pt Nanoelectrodes: Evidence of Surface Diffusion and Spillover

Dongping Zhan, Jeyavel Velmurugan, and Michael V. Mirkin*

Department of Chemistry and Biochemistry, Queens College - CUNY, Flushing, New York 11367

Received April 10, 2009; E-mail: mmirkin@qc.cuny.edu

Abstract: Nanoelectrochemical approaches were used to investigate adsorption/desorption of hydrogen on Pt electrodes. These processes, which have been extensively studied over the last century, remain of current interest because of their applications in energy storage systems. The effective surface area of a nanoelectrode was found to be much larger than its geometric surface area due to surface diffusion of adsorbed redox species at the Pt/glass interface. An additional peak of hydrogen desorption was observed and attributed to the spillover of hydrogen from the Pt surface into glass. The results were compared to those obtained for underpotential deposition of copper on Pt nanoelectrodes.

Introduction

The electrolysis of water, which was first observed by Volta in the beginning of the 19th century, is probably the best studied electrochemical process. At a Pt working electrode, water can be either oxidized at positive potentials to produce oxygen or reduced at negative potentials to produce hydrogen. Extensive studies of both hydrogen and oxygen evolution reactions focused on their kinetics,[1] catalysis,[2] and numerous applications including energy storage.[3] Adsorption of hydrogen and oxygen species occurs at less negative (hydrogen) and positive (oxygen) potentials than their evolution processes. Voltammetry in acidic solution is a standard technique used for electrode characterization, and a typical cyclic voltammogram (CV) at a large (i.e., millimeter-sized) Pt electrode exhibits several pairs of peaks corresponding to adsorption/desorption of hydrogen and oxygen-containing species (Figure 1A).[4] The characteristic value of charge density associated with a monolayer of hydrogen adsorbed on polycrystalline platinum ($210 \ \mu C/cm^2$) is widely used to determine the true (microscopic) surface area of Pt electrodes.[5] The ratio of the microscopic surface area to the geometric area (A_m/A_g) gives the roughness factor (ρ).[6]

An important process related to hydrogen adsorption is the spillover, i.e., migration of the chemisorbed hydrogen from the metal electrode (or catalyst) onto the support surfaces. Known for decades,[7] this phenomenon recently attracted significant attention because of its implications for hydrogen storage.[8] The
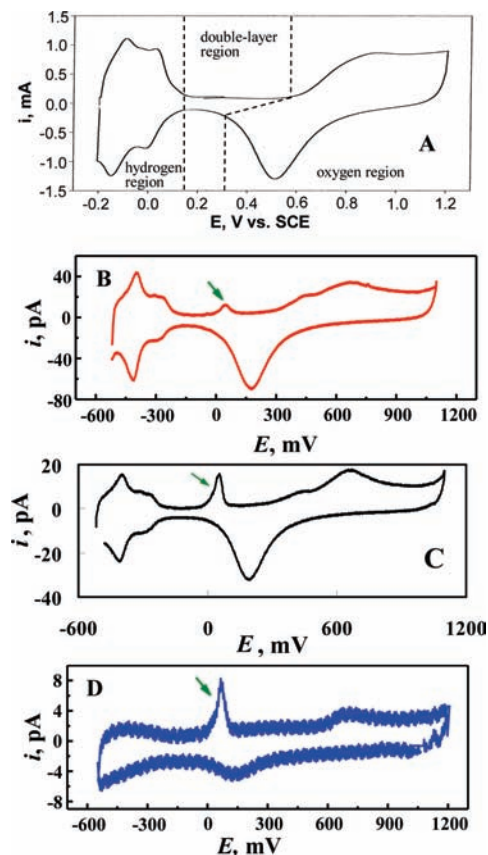

Figure 1. Cyclic voltammograms obtained in 0.5 M H_2SO_4 solution at (A) a macroscopic Pt electrode (A_m = 5.47 cm^2)[4] and (B–D) Pt nanoelectrodes. a = 103 nm (B), 52 nm (C), and 11 nm (D). ν, mV/s = 100 (A) and 500 (B–D).

mechanisms of hydrogen spillover onto various amorphous and crystalline substrates surfaces including oxides,[9] activated

(1) Vetter, K. J. *Electrochemical kinetics: theoretical and experimental aspects*; Academic Press: New York, 1967.
(2) Electrocatalysis. *Frontiers of Electrochemistry*; Lipkowski, J.; Ross, P. N., Eds.; Wiley-VCH: Weinheim, 1998; Vol. 4.
(3) Haas, O.; Cairns, E. J. Electrochemical energy storage. In *Annual reports on the progress of chemistry*; The Royal Society of Chemistry: London, 1999; Vol. 95C, pp 163–197.
(4) Attard, G. S.; Bartlett, P. N.; Coleman, N. R. B.; Elliott, J. M.; Owen, J. R.; Wang, J. H. *Science* **1997**, *278*, 838.
(5) Trasatti, S.; Petrii, O. A. *Pure Appl. Chem.* **1991**, *63*, 711.
(6) Bard, A. J.; Faulkner, L. R. *Electrochemical Methods: Fundamentals and Applications*; John Wiley & Sons, Inc.: New York, 2001.
(7) Robell, A. J.; Ballou, E. V.; Boudart, M. *J. Phys. Chem.* **1964**, *68*, 2748.
(8) Yang, R. T.; Wang, Y. *J. Am. Chem. Soc.* **2009**, *131*, 4224.

(9) Conner, W. C.; Falconer, J. L. *Chem. Rev.* **1995**, *95*, 759.

carbon,[10] zeolites,[11] and metal organic frameworks[12] have been investigated; however, little is known about its spillover in glass.

Here we employ nanometer-sized Pt electrodes to probe hydrogen adsorption/desorption processes. An electrode of this type with a radius, $a \geq 5$ nm can be produced by pulling a Pt microwire into a glass capillary with the help of a laser pipet puller.[13a] After pulling, the metal wire is completely sealed into glass, and its nanometer-sized tip can be exposed by gentle polishing under video microscopic control. The geometry of polished nanoelectrodes was thoroughly characterized by a combination of voltammetry, scanning electron microscopy, and scanning electrochemical microscopy (SECM). It was shown that the radius value determined from steady-state voltammetry is close to the effective radius of the conductive disk. The absence of detectible solution leakage through the glass seal was also demonstrated.[13] An important advantage of well-characterized disk-type nanotips is the possibility of quantitative data analysis.

A fundamental question in nanoelectrochemistry is whether any unexpected phenomena may occur at nanointerfaces that cannot be observed in macroscopic electrochemical systems.[13c,14,15] Below we report unusual features of hydrogen adsorption/desorption processes, which could be observed at Pt nanoelectrodes, but not at macroelectrodes, because of the very small surface area of the metal/solution interface.

Experimental Section

Chemicals. Ferrocenemethanol (FcCH$_2$OH, 97%) from Aldrich (Milwaukee, WI) was recrystallized twice from acetonitrile. Hexaammineruthenium(III) chloride (Ru(NH$_3$)$_6$Cl$_3$, 99%) was obtained form Strem Chemicals (Newburyport, MA). H$_2$SO$_4$ from Aldrich (Milwaukee, WI), CuSO$_4$ from Mallinckrodt Inc. (Paris, KY), and KCl from Fisher Scientific Co. (Fair Lawn, NJ) were used as received. Aqueous solutions were prepared from deionized water (Milli-Q, Millipore Co.).

Electrodes and Electrochemical Cells. The fabrication of the laser-pulled Pt nanoelectrodes was described previously.[13a] Briefly, an annealed 25-μm Pt wire (Goodfellow) was pulled into a borosilicate capillary (Drummond; 1.0-mm o.d., 0.2-mm i.d.) under vacuum with the help of a Sutter P-2000/G laser pipet puller. The pulled electrodes were polished on 50 nm lapping tape under video microscopic control and washed by distilled water. The effective radius of an electrode was evaluated from steady-state voltammetry, and only electrodes producing well-shaped sigmoidal voltammograms of 1 mM FcCH$_2$OH at a scan rate, $v = 50$ V/s were used for experiments. A Ag/AgCl reference electrode was used for FcCH$_2$OH and Ru(NH$_3$)$_6$Cl$_3$ voltammetry. Experiments in H$_2$SO$_4$ and CuSO$_4$ solutions were performed with a coated-wire Ag/Ag$_2$SO$_4$ reference to avoid the contact of Pt surface with Cl$^-$.

Instrumentation and Procedures. Chronoamperometric and SECM measurements were performed using a home-built SECM instrument that includes an EI-400 bipotentiostat (Ensman Instruments, Bloomington, IN).[17] Cyclic voltammograms were obtained using either an EI-400 bipotentiostat or a BAS-100B electrochemical analyzer (Bioanalytical Systems, West Lafayette, IN). To remove oxygen, the solutions were purged with high-purity nitrogen before and during the experiments. All experiments were performed at

room temperature (23 ± 2 °C) inside a Faraday cage. Unless otherwise specified, CVs of hydrogen adsorption/desorption show the second or subsequent potential cycles, which are essentially indistinguishable from each other (steady-state response) but different from the first potential sweep.

Results and Discussion

Figure 1B shows a CV of 0.5 M H$_2$SO$_4$ solution at a 103-nm-radius Pt electrode. With the well-defined hydrogen, double-layer, and oxygen regions, the CV shape is quite similar to that in Figure 1A, which was obtained at a millimeter-sized electrode.[4] However, the measured pA-range current is much higher than expected for $a = 103$ nm and the potential sweep rate, $v = 500$ mV/s. The electrode surface area, $A_m = 7.8 \times 10^6$ nm^2, was found by integrating the reduction current in the hydrogen adsorption region. The corresponding effective roughness factor, RF = 234 is incomparably larger than the intrinsic roughness factor, $\rho \approx 2$, typical of polished Pt electrodes.[6] Assuming cylindrical geometry of the sealed in glass Pt wire, the length of the portion of the wire at which the oxidation/reduction of water takes place must be $l \approx 12$ μm to account for the apparent surface area of 7.8×10^6 nm^2.

Another surprising feature in Figure 1B is a small anodic peak in the double-layer region marked by the green arrow (the peak potential, $E_p \cong 50$ mV vs Ag|Ag$_2$SO$_4$ reference; below it is referred to as "DL peak" because of its location in the double-layer region). The smaller the electrode radius the more prominent this peak becomes in comparison to other voltammetric waves (cf. Figures 1B–D). The effective RF value also increases with decreasing a (see above).

A simple explanation for the unrealistically large RF values found for laser-pulled Pt nanoelectrodes would be solution leakage through the Pt/glass seal. However, the experiments conducted with various redox species dissolved in solution showed no evidence of leakage. Figure 2 (inset) shows two CVs of 1 mM FcCH$_2$OH at the same 52-nm electrode, which was also used to obtain a CV in Figure 1C. The difference between the voltammograms obtained at $v = 50$ mV/s (pink) and 50 V/s (blue) is only in a larger charging current observed with a higher scan rate. There is no indication of a peak that would be expected if a narrow solution-filled cavity existed inside the glass sheath. Similar fast scan voltammograms were obtained for a number of polished Pt nanoelectrodes, but no peak-shaped CVs were obtained even with much higher concentrations of redox species (e.g., 25 mM Ru(NH$_3$)$_6$$^{3+}$; not shown).

Additional evidence against electrode leakage comes from the SECM approach curves (Figure 2), which show an excellent agreement between the experimental data (symbols) and the theory (solid curve) even at very close tip/substrate separation
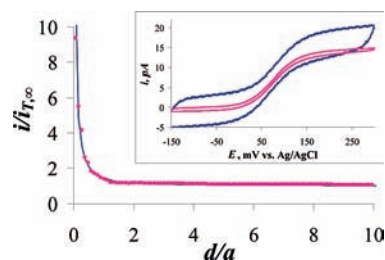
(10) Li, Y.; Yang, R. T. *J. Am. Chem. Soc.* **2006**, *128*, 12410.

(11) Salzer, R.; Dressler, J.; Steinberg, K. H.; Roland, U.; Winkler, H.; Klaeboe, P. *Vib. Spectrosc.* **1991**, *1*, 363.

(12) Miller, M. A.; Wang, C.-Y.; Merrill, G. N. *J. Phys. Chem. C* **2009**, *113*, 3222.

(13) (a) Sun, P.; Mirkin, M. V. *Anal. Chem.* **2006**, *78*, 6526. (b) Sun, P.; Mirkin, M. V. *Anal. Chem.* **2007**, *79*, 5809. (c) Sun, P.; Mirkin, M. V. *J. Am. Chem. Soc.* **2008**, *130*, 8241.

(14) Smith, C. P.; White, H. S. *Anal. Chem.* **1993**, *65*, 3343.

(15) He, R.; Chen, S.; Yang, F.; Wu, B. *J. Phys. Chem. B* **2006**, *110*, 3262.

Figure 2. Experimental (symbols) and theoretical (solid line) approach curves for a 52 nm Pt electrode approaching an evaporated Au substrate. The tip current is normalized by its value in the bulk solution ($i_{T,\infty}$). The insert shows CVs at the same electrode; $v = 50$ mV/s (pink) and 50 V/s (blue). Solution contained 1 mM FcCH$_2$OH and 100 mM NaCl.

distances (d; e.g., the shortest distance in Figure 2 is $d \cong 0.1a$ = 5.2 nm). Importantly, the fit was obtained with the same a = 52 nm that was found from the CV (pink curve in the Figure 2 inset). Such an agreement would not be possible if the insulating glass sheath were leaking. This conclusion is in accordance with ref 16 where no leakage was revealed by extensive characterization of glass-sealed Pt nanoelectrodes, and with our previous results.[13]

Since the shape of the entire nanoelectrode CV (including the peaks present in both hydrogen and oxygen regions; Figures 1B and 1C) is very similar to that of the CV obtained at a large Pt electrode (Figure 1A), one has to conclude that the A_m value is the same for both hydrogen adsorption/desorption and oxide formation/reduction processes. This is in agreement with the notion that the same redox species, water, participates in both processes.[18] Unlike $FcCH_2OH$ and $Ru(NH_3)_6Cl_3$, water molecules adsorb on the Pt surface[19] and can travel on it via surface diffusion.[20] The surface diffusion of water along the Pt/glass boundary results in a the formation of an aqueous film covering a micrometer-long portion of the Pt wire; hence, a dramatic increase in the A_m and RF values obtained from Figures 1B−D. In the absence of this effect (e.g., when surface diffusion is negligibly slow or the insulated portion of the metal surface is chemically passivated), the nanoelectrode surface area found from oxidation/reduction of the adsorbed molecular monolayer is similar to the area calculated from the diffusion current of redox species dissolved in solution.[21]

The unusual DL peak in Figures 1B−D can be recorded by scanning the electrode potential between the double-layer region (e.g., ~200 mV vs Ag/Ag$_2$SO$_4$) and hydrogen region, as shown in Figure 3; therefore, it is not related to oxide formation/reduction. However, this peak does not appear unless the negative limit of the potential scan is in the hydrogen region (i.e., the switching potential, $E_\lambda \lesssim -250$ mV).

One may notice some similarity between the DL peak and a sharp peak that appeared on voltammograms of Pt (111) electrodes in H$_2$SO$_4$ and H$_3$PO$_4$ solutions and was attributed to anion adsorption.[22] However, the adsorption peaks in ref 22 were reversible, in contrast with the totally irreversible DL peak. Another important difference is that the DL peak appears only after the Pt electrode potential was made sufficiently negative to induce hydrogen adsorption. The DL peak was also present in CV's recorded in perchlorate solutions (not shown), in which no anion adsorption peak was observed.[22]

Table 1 presents additional evidence that the DL peak is due to hydrogen desorption. For three different nanoelectrodes, the cathodic charge corresponding to hydrogen adsorption (Q_a) is larger than the Q_d value found by integrating the anodic current in the hydrogen region. However, a very close agreement between the adsorption and desorption charges, within 5%, can be obtained by adding the Q_{DL} value (i.e., the integral of the current under the DL peak) to Q_d. To our knowledge, the DL
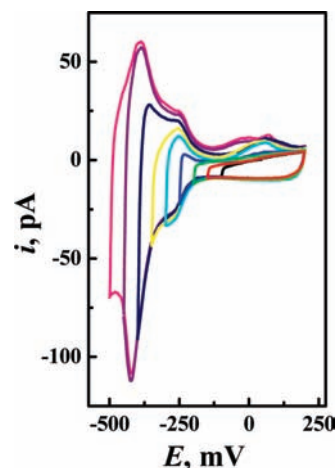

Figure 3. Effect of the negative potential scan limit on CVs of hydrogen adsorption/desorption at a 140-nm Pt electrode in 0.5 M H$_2$SO$_4$ solution. The potential was swept between +200 mV and different values of E_λ (mV): −500 (pink), −450 (purple), −400 (dark blue), −350 (yellow), −300 (turquoise), −250 (blue), −200 (green), −150 (red), and −100 (black). ν = 200 mV/s.

peak has not been observed at macroscopic electrodes, and it becomes more prominent as a decreases (Figures 1B−D and Table 1). This irreversible peak (there is no corresponding cathodic peak) can be attributed to hydrogen desorption at the Pt/glass interface.

Table 1. Anodic and Cathodic Charges and Effective Roughness Factors Obtained from CVs of Hydrogen Adsorption/Desorption (0.5 M H$_2$SO$_4$) and Stripping of Underpotentially Deposited Copper (10 mM CuSO$_4$ + 0.5 M H$_2$SO$_4$) at Pt Nanoelectrodes

electrode	a, nm	hydrogen adsorption/desorption				UDP of copper	
		Q_a, pC	Q_d, pC	Q_{DL}, pC	RF$_H$	Q_{Cu}, pC	RF$_{Cu}$
1	38	7.9	5.7	1.9	829	15.9	855
2	86	24.5	21.8	2.1	503	45.3	473
3	140	64.1	59.2	6.3	491	113.9	448

In all voltammograms discussed above (Figures 1B−D and 3), the successive potential cycles (starting with the second cycle; the first potential sweep is always somewhat different) produced almost indistinguishable current responses. This indicates that the Pt surface area covered by the water monolayer was essentially constant and time-independent. The corresponding steady-state RF can be expressed as

$$RF = A_m/A_g = (\pi a^2 + 2\pi al)/\pi a^2 = 1 + 2l/a \qquad (1)$$

and, thus, the effective length of the Pt wire covered by the water film is

$$l = a(RF - 1)/2 \qquad (2)$$

Although eq 2 does not take into account the roughness of Pt surface, it should still provide a realistic estimate for l because the RF values of several hundred are incomparably larger than $\rho \approx 2$ expected for polished Pt.[6] From RF values for hydrogen adsorption in Table 1 one obtains $l = 25 \pm 8$ μm. This distance may represent the length of the wire portion sealed in glass. The oxidation/reduction of water at the Pt/glass interface was observed recently.[23] The variations in l in Table 1 are quite significant (within the factor of 2), and they may be even larger

(16) Zhang, B.; Galusha, J.; Shiozawa, P. G.; Wang, G.; Bergren, A. J.; Jones, R. M.; White, R. J.; Ervin, E. N.; Cauley, C. C.; White, H. S. *Anal. Chem.* **2007**, *79*, 4778.

(17) Laforge, F. O.; Velmurugan, J.; Wang, Y.; Mirkin, M. V. *Anal. Chem.* **2009**, *81*, 3143.

(18) Pletcher, D.; Sotiropoulos, S. *J. Chem. Soc., Faraday Trans.* **1994**, *90*, 3663.

(19) Velasco, J. G. *Chem. Phys. Lett.* **1999**, *313*, 7.

(20) Spohr, E. *J. Phys. Chem.* **1989**, *93*, 6171.

(21) Watkins, J. J.; Chen, J.; White, H. S.; Abruña, H. D.; Maisonhaute, E.; Amatore, C. *Anal. Chem.* **2003**, *75*, 3962.

(22) Herrero, E.; Franaszczuk, K.; Wieckowski, A. *J. Phys. Chem.* **1994**, *98*, 5074.

(23) Velmurugan, J.; Zhan, D.; Mirkin, M. V. Manuscript in preparation.

for nanoelectrodes prepared using different fabrication methodologies or different pulling programs.

Micrometer-range l values indicate that the effect of surface diffusion of water should be observable not only at nanoelectrodes but also at micrometer-sized electrodes (assuming $l = 25$ μm, one obtains RF = 11 for $a = 5$ μm and RF = 1.05 for $a = 1$ mm). To check this hypothesis, we obtained CVs of hydrogen adsorption/desorption at a 12.5-μm radius glass-sealed Pt disk electrode produced by using standard procedures for microelectrode fabrication (i.e., heat-sealing without pulling[24]). The obtained RF value of 18 shows that the surface diffusion effect is indeed significant for micrometer-sized electrodes. $l \approx 100$ μm calculated from eq 2 for this electrode was comparable to the microscopically observed length of the glass-sealed portion of the Pt wire.

CVs of hydrogen adsorption/desorption at micrometer-sized Pt electrodes were presented previously in ref 18. The charge found by integrating the cathodic current in the hydrogen region of the CV obtained at the 5-μm radius Pt disk electrode (Figure 2 in ref 18) corresponds to $A_m \approx 4 \times 10^3$ μm^2 and RF ≈ 50. Other CVs in ref 18 yield similar RF values. (The A_m values are not reported in ref 18 which is largely concerned with the effect of pH on hydrogen peak potentials).

Underpotential deposition (UPD) of copper at Pt nanoelectrodes has been widely employed to evaluate A_m using a conversion factor of 410 μC/cm^2 for polycrystalline Pt.[5,25,26] To facilitate the comparison of the A_m and RF values, we obtained CVs of the copper stripping from the same nanoelectrodes that were employed in hydrogen adsorption/desorption measurements (Table 1). Unlike hydrogen adsorption/desorption processes, which produce steady-state CVs without preaccumulation, the height of the copper stripping peak increases significantly if the electrode is held at a potential sufficiently negative to induce UPD of Cu before the anodic scan. Several stripping voltammograms shown in Figure 4 were obtained at the same 86-nm radius Pt electrode after holding it at -320 mV vs Ag|Ag$_2$SO$_4$; the holding time (t) was varied between 10 s and 4 min. The corresponding charge (i.e., the area under the stripping peak plotted in the inset as a function of t) initially increased with t and leveled off at $t \cong 120$ s. Thus, it takes ~2 min to form a complete monolayer of copper adatoms on the entire Pt surface. Similar behavior was reported by Elliott et al.[26] In their experiments, up to 5 min holding time was required to achieve complete coverage of the nanostructured Pt microelectrode surface by underpotentially deposited Cu while it took only a few seconds for nearly complete coverage of a polished Pt macroelectrode. This difference was attributed to the hindered transport of Cu^{2+} ions through the porous nanostructure.[26] In our case, the deposition time required to attain the complete coverage is determined by the rate of surface diffusion of copper adatoms on the Pt/glass interface. Unlike Cu adatoms that have to be generated in situ by holding a Pt electrode at a negative potential, an aqueous monolayer is formed on the Pt surface immediately after its immersion in solution.

The charge (Q_{Cu}) and corresponding RF$_{Cu}$ values in Table 1 were obtained from copper stripping voltammograms recorded after 2-min long deposition at $E = -320$ mV. The remarkably

(24) Wightman, R. M.; Wipf, D. O. In *Electroanalytical Chemistry*; Bard, A. J., Ed.; Marcel Dekker: New York, 1989; Vol. 15, p 267.
(25) Machado, S. A. S.; Tanaka, A. A.; Gonzalez, E. R. *Electrochim. Acta* **1991**, *36*, 1325.
(26) Elliott, J. M.; Birkin, P. R.; Bartlett, P. N.; Attard, G. S. *Langmuir* **1999**, *15*, 7411.
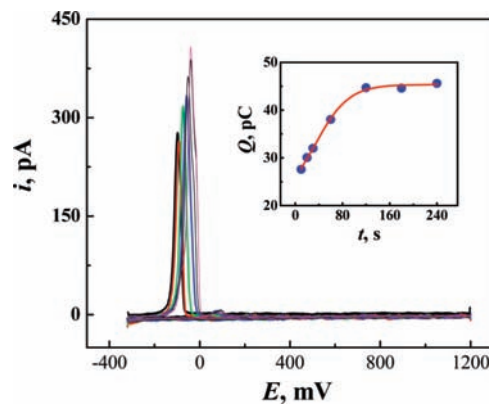
Figure 4. CVs of stripping of underpotentially deposited Cu from 86-nm radius Pt electrode. Before stripping, the electrode was held at -320 mV vs Ag|Ag$_2$SO$_4$ for (from bottom to top): 10 s, 20 s, 30 s, 1 min, 2 min, 3 min, and 4 min. $v = 500$ mV/s. The insert shows the charge obtained from each stripping peak as a function of holding time. The solid curve is shown as a guide.

close agreement (within <10%) between the RF values obtained from hydrogen and copper voltammograms at each nanoelectrode suggests that the same surface area (A_m) was covered by both species. Nevertheless, major differences between these processes became apparent when we tried to preaccumulate hydrogen by holding the electrode potential at -450 mV before obtaining a CV (Figure 5). The most prominent feature in Figure 5 is a very large DL peak whose height increased with holding time, t. A very high peak current (at $t = 30$ min, it was >100 times higher than without preaccumulation) obscures other voltammetric features whose magnitude was essentially independent of t. Unlike Cu UPD, the Q vs t dependence (the inset in Figure 5; obtained by integrating the anodic current in the hydrogen and double-layer regions) has not leveled off after 2 min. The very large charge values in Figure 5 (inset) and its continuing increase even at $t \geq 30$ min cannot be attributed to adsorption/desorption of a monolayer of hydrogen.
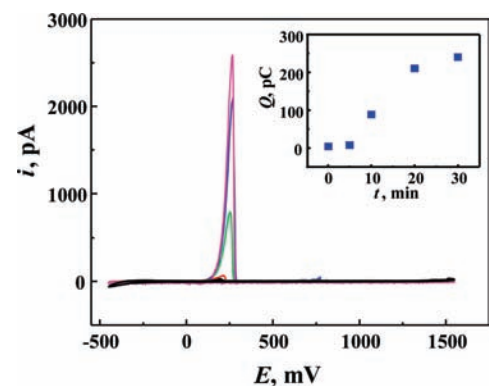

Figure 5. CVs recorded in 0.5 M H$_2$SO$_4$ solution after holding a 38-nm Pt nanoelectrode at -450 mV vs Ag|Ag$_2$SO$_4$ quasi-reference. t, min (from bottom to top): 0.1, 5, 10, 20, 30. $v = 500$ mV/s. Insert: dependence of the anodic charge vs t obtained from the same CVs.

The data in Figure 5 suggest that most of hydrogen generated when the electrode was held at -450 mV was transferred into the glass phase via spillover from the Pt surface. During the subsequent potential sweep in the positive direction, the accumulated hydrogen diffuses to the Pt surface and gets reoxidized on it (Figure 6). This process is responsible for the DL peak. The DL peak cannot be recorded at a conventional-

size Pt electrode because of its large surface area and high Faradaic and charging currents flowing at the metal/solution interface. This peak becomes apparent when the electrode radius is smaller than ∼200 nm (Figure 1B).
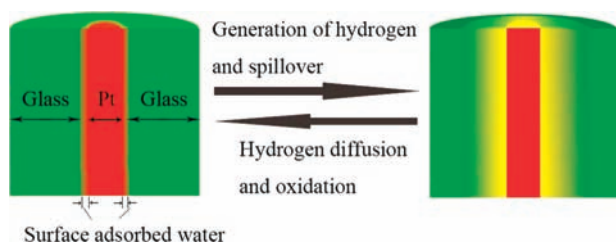

Figure 6. Schematic representation of hydrogen generation in the adsorbed water film on the negatively biased Pt surface, its spillover into glass, diffusion within the glass phase, and oxidation on Pt surface at positive potentials.

To test this model, we compared the charges corresponding to accumulation and oxidation cycles of hydrogen and copper at the same nanoelectrode. The integration of chronoamperometric reduction current (Figure 7A) recorded over the 5 min period after stepping the Pt nanoelectrode potential from 200 mV to −450 mV yielded $Q_a = 354$ pC. This number is ∼10 times larger than the total hydrogen desorption charge ($Q = Q_d + Q_{DL} = 14.2$ pC + 24.6 pC = 38.8 pC) obtained from Figure 7B. The ∼90% loss of the accumulated hydrogen results from its spillover from Pt and bulk diffusion into the glass phase. The UPD/stripping of copper on the same nanoelectrode (Figures 7C and 7D) produced completely different results: the stripping charge (110.9 pC) was very similar to the charge obtained from the deposition transient (114.8 pC), as expected in the absence of spillover effects.[5]

Apparently, the spillover of hydrogen from Pt onto glass is a spontaneous process, which is driven not only by concentration gradient but also by the free energy of hydrogen chemisorption on glass. The reverse process is not spontaneous, and because of its overpotential the DL peak appears at significantly more positive potentials than regular hydrogen desorption peaks. Somewhat similar voltammetric responses were reported previously for hydrogen spillover from the Pt/Nafion interface.[27] The observed spillover of adsorbed hydrogen is different from physicosorption of H_2 gas on glass. The differences between chemisorption and physicosorption of hydrogen have previously been discussed for materials other than glass.[28] The latter process would not produce a significant shift in desorption peak potential.

Conclusions

We used nanoelectrochemical approaches to reinvestigate well-studied processes: hydrogen adsorption/desorption at polycrystalline Pt. A very small surface area of a nanoelectrode exposed to solution allowed us to observe unusual features of
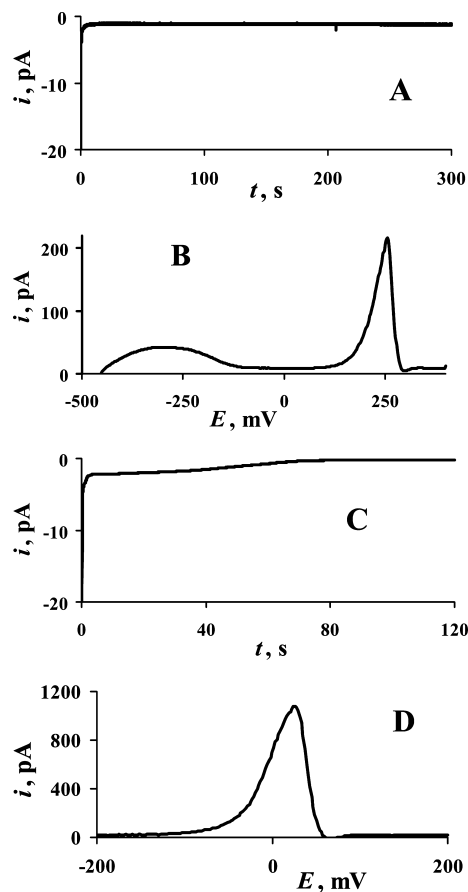
(27) Tu, W.; Liu, W.; Cha, C.; Wu, B. *Electrochim. Acta* **1998**, *43*, 3731.
(28) Makowski, P.; Thomas, A.; Kuhn, P.; Goettmann, F. *Energy Environ. Sci.* **2009**, *2*, 480.

Figure 7. Chronoamperograms of hydrogen adsorption (A) and copper UPD (C), and anodic voltammograms of hydrogen (B) and copper stripping (D) recorded at the same 129-nm raduis Pt electrode. Solution contained 0.5 M H_2SO_4 and (C, D) 10 mM $CuSO_4$. The potential was stepped from +200 mV to −450 mV (A) and from +200 mV to −320 mV (C) vs Ag|Ag_2SO_4. (B, D) $\nu = 500$ mV/s.

these reactions, which would not be accessible by conventional-size electrochemical probes. In the case of glass-sealed electrodes, a monolayer of adsorbed species can form at the metal/glass interface thus greatly increasing the effective surface area. This effect was demonstrated for a monolayer of adsorbed water and for copper underpotentially deposited on Pt.

The spillover of hydrogen adatoms from the Pt/glass interface results in accumulation of hydrogen inside the glass phase. The subsequent oxidation of the spilled hydrogen at Pt during the anodic potential sweep results in the appearance of an unusual peak in the double-layer region. The extent of hydrogen spillover in glass and potential implications of this phenomenon for hydrogen storage are currently being explored in our laboratories.